Alinteri J. of Agr. Sci. (2021) 36(1): 486-499
e-ISSN: 2587-2249
info@alinteridergisi.com

http://dergipark.gov.tr/alinterizbd
http://www.alinteridergisi.com/
DOI:10.47059/alinteri/V36I1/AJAS21070

RESEARCH ARTICLE

Coastal Depth Extraction from Satellites Images

Nur Syahirah Hashim[1] • Khairul Nizam Tahar[2] • Wiwin Windupranata[3] • Saiful Aman Hj Sulaiman[4*]

[1]*Master of Science, Built Environment Student, Faculty of Architecture, Planning & Surveying, MARA University of Technology Malaysia Shah Alam, Selangor, Malaysia.*

[2]*Senior Lecturer, Faculty of Architecture, Planning & Surveying, MARA University of Technology Malaysia Shah Alam, Selangor, Malaysia.*

[3]*Lecturer & Researcher, Department of Geodesy and Geomatics Engineering, Institute Technology Bandung, Indonesia.*

[4*]*Senior Lecturer, Faculty of Architecture, Planning & Surveying, MARA University of Technology Malaysia Shah Alam, Selangor, Malaysia.*

ARTICLE INFO

Article History:
Received: 28.03.2021
Accepted: 02.05.2021
Available Online: 21.06.2021

Keywords:
Survey and Mapping Malaysia (DSMM)
Single-beam echo sounder (SBES)
Satellite-Derived Bathymetry (SDB)

ABSTRACT

The problems in bathymetry measurement often have gaps or 'holes' within the data. As a result, hydrographic surveyors often have sparse data, and even though the data is dense and equal distances, there is still a gap in time. This paper present coastal depth extraction from satellite images. The problem encountered during the bathymetry derivation process and the problem related to the space, distribution and quantity of the Single-beam echo sounder (SBES) data. Therefore, the idea of using spatial interpolation could be a suitable approach in solving the problems. This study intends to produce Satellite-Derived Bathymetry (SDB) from Landsat 8 images at Pantai Tok Jembal, Terengganu, Malaysia. The proposed method by first interpolating the SBES point in the calibration data using spatial predictors, i.e. Inverse Distance Weightage, Thin-Plate Spline, Spline with Tension, Universal Kriging, Natural Neighbor, and Topo to Raster. Second, the raster output created from the interpolation process then converts into the point shapefile. Third, intersect function use to eliminate the point whereby not in the domain. Finally, the newly generated SBES points in calibration data ready to apply at the SDB computation process, generating SDB. In continuation, a comparative analysis conducted between six SDB results generated using each different newly generated calibration data. The result indicates SDB utilizes with Universal Kriging-newly generated calibration data (RMSE: 0.718 m) was the best result. To summarise, this study has successfully attained the research objectives by utilizing the newly generated calibration data in generating SDB. The task of spatial interpolation recreates the SBES data from irregular space and short data to uniform space and long data, which facilitate in pixel to point value extraction and help refine the bathymetry derivation process. Furthermore, the proposed method suitable to be used when the data are not applicable or limited.

Please cite this paper as follows:

Hashim, N.S., Tahar, K.N., Windupranata, W. and Sulaiman, S.A.H. (2021). Coastal Depth Extraction from Satellites Images. *Alinteri Journal of Agriculture Sciences, 36*(1): 486-499. doi: 10.47059/alinteri/V36I1/AJAS21070

Introduction

The problems in bathymetry measurement often have gaps or 'holes' within the data. As a result, hydrographic surveyors often have sparse data, and even though the data is dense and equal distances, there is still a gap in time. A single-beam echo sounder (SBES) system, a bathymetric acquisition technique, is used to provide the bathymetric data.

Other than work-related, in research studies, SBES data commonly use in Satellite-derived Bathymetry (SDB) related studies [21]-[26], [32], [36]-[37]. In this study, SBES data as a ground truth data, use in generating SDB at Pantai Tok Jembal, Terengganu, Malaysia and the importance of the data use especially during the SDB computation process. However, the major problem in SBES data provided is in sparse and irregular space, creates a data gap and 'holes' within data, which leads to missing important bathymetry information.

* Corresponding author: Saiful Aman Hj Sulaiman

Based on the SBES data provided, 62% of the SBES survey area (6.66 km^2) at Pantai Tok Jembal cover the bathymetry information, while the rest 38% were not. The significant contribution of 38%, missing important bathymetric information is firstly from the uneven and irregular sampling. The measurement using SBES system, the depth of the seafloor is measured using the two-way journey time of a sound wave sent to and from the seafloor [39], and SBES disadvantages are only has a small seabed fraction [7], i.e., the measurement using a single transducer, ping by ping at a time, hence the bathymetry data collected in a sparse interval. Besides, the speed and time variations during the ship measurement led to the observation taken at different positions each time, thus creating an inconsistent distance between the data point. Secondly, there are variations in the ship track's design, with several sounding line and crossline created. Surveyor tends to minimize the line to reduce time and cost, leading to a gap of data interval. Thirdly, a possible error can be the equipment failure during onboard measurement. The unintended or intended system shutdown or weak signals from the system leaves an information gap [8]. And finally, unintended 'holes' created within the SBES data, whereby a shallow area located at 0.5 km from the Pantai Tok Jembal shoreline. This area has narrow space navigation, i.e., the small space between the bottom of the ship or the instrument with a seabed area. Space navigation different in each variation design of ship use. The smaller the ship, the better to use but still limited to the particular depth extent, and because the ship cannot access a shallower area, leave the area unmeasured. Furthermore, it is necessary to avoid the shallower area to avoid ship and instrument grounding to keep the safe navigation.

This paper present coastal depth extraction from satellite images. The problem encountered during the bathymetry derivation process whereby the pixel to point value extraction undertaken. The irregular space of SBES data and the 15 m resolution of Landsat images, causes more than one SBES point with different depth value fit into the one Landsat pixel, thus, due this problem create uncertainty. Also, the unintended 'holes' within the SBES data, reducing quite an amount of data, which is essentially needed, since SBES data use as ground truth data. The lack of ground truth data among the obstacles faced in the bathymetry derivation process. When the data is insufficient, the bathymetry estimation works well as a rough estimation as happen in [13] study. Besides, according to [38], the accuracy depended on the quality and quantity of ground truth data. In terms of quantity of data, a study conducted by [19] compares the accuracy of Lyzenga's extension method evaluating with Acoustic Doppler Current Profiler (ADCP) and Multi-Beam Echo Sounder (MBES). Two evaluations made, firstly with 200 points, and secondly, with 500 points of ground truth data. The result concludes that the increasing number of ground truth data can improve and gives a better result. While, in terms of quality of data, completing the data quality traits is a reliable inaccuracy, comprehensive in information, relevance in information, and timelessness [31]. On top of that, the way data supposed to be dense, regularly space and long, and this has been explained by [8], whereby most analysis procedures are designed for long and dense sample data along with equally spaced measurement in time or space. Besides, the wealth of information applies to regularly spaced and abundant measurement. Therefore, the idea of using spatial interpolation could be a suitable approach in solving the problems.

This study intends to produce SDB from Landsat 8 images at Pantai Tok Jembal, Terengganu, Malaysia, within the extended survey area (49.69 km^2) [25]-[26], using bathymetry algorithm, Log-ratio Transform. A bit modification of the bathymetry derivation process whereby at the SDB computation process. The proposed method by first interpolating the SBES point in the calibration data using spatial predictors, i.e. Inverse Distance Weightage, Thin-Plate Spline, Spline with Tension, Universal Kriging, Natural Neighbor, and Topo to Raster. Second, the raster output created from the interpolation process then converts into the point shapefile. Third, intersect function use to eliminate the point whereby not in the domain. Finally, the newly generated SBES points in calibration data ready to apply at the SDB computation process, generating SDB. The proposed method uses spatial predictors interpolating the SBES points in the calibration data. The task of spatial interpolation recreates the SBES data from irregular space and short data to uniform space and long data, which facilitate in pixel to point value extraction and help refine the bathymetry derivation process.

Furthermore, three objectives will guide this paper: first, to evaluate the spatial interpolation method use in interpolating calibration data. Second, generating SDB of the extended area using newly generated calibration data (produced from a different spatial predictor). Third, to conduct an accuracy assessment of SDB of the extended area. For the analysis, there are three stages of analysis conducted connecting the objective in this research: firstly, evaluate the pattern error of spatial prediction in the production of newly generated calibration data. Secondly, the evaluation of SDB generated using newly generated calibration data. Thirdly, evaluate the result of accuracy assessment of SDB at the extended area.

Material & Methods

Study Area & Data Used

Pantai Tok Jembal locates at Terengganu, Malaysia, at approximately 5°24'00" N, 103°00'00" E [25]-[26]. This location was chosen as the study area to derive water depth—the study area located close to the Sultan Mahmud Shah Airport and the University of Malaysia Terengganu. Apart from local or tourist attractions, this area has 400 households living near the coastal area from Pantai Tok Jembal to Batu Rakit, with a distance of 3 km [18].

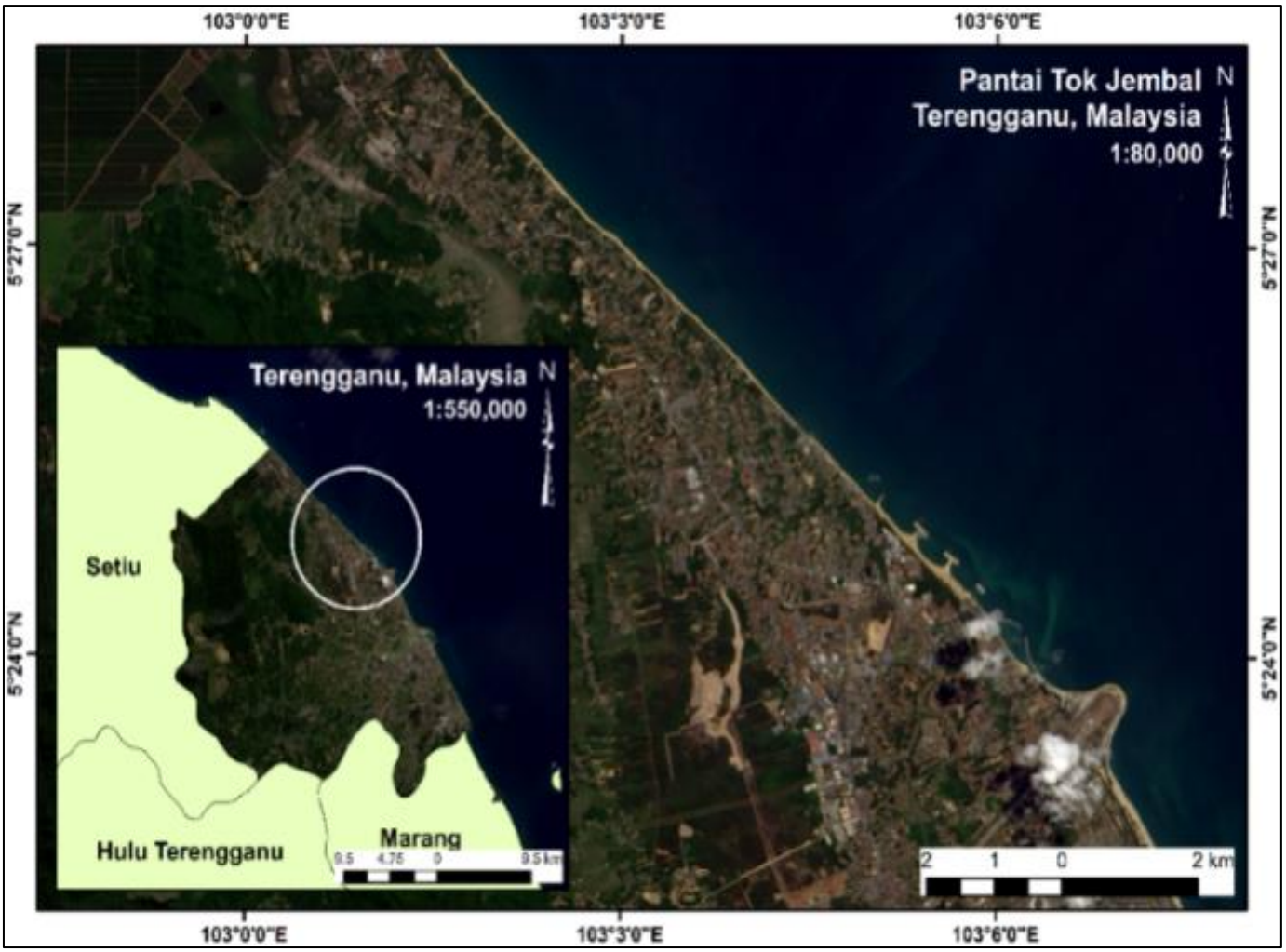

Figure 1. Showing a study area, Pantai Tok Jembal, Terengganu, Malaysia (latitude: 05°24'00" N, longitude: 103°00'00"E)

In continuation, SBES data, Landsat 8 images and tidal data [25]-[26] are three types of data used in this study. First, the SBES data collected using SONARLITE Portable Single Beam Echo Sounder (vertical) and Astech SP80 Global Navigation Satellite System (GNSS) receiver (horizontal), surveyed in the year 2017 and this data provided by the Department of Irrigation and Drainage Malaysia (DID). The horizontal and vertical accuracy was ± 0.3 cm [34] and ± 2.5 cm [33], and the total SBES points measured were 18283 with a range of depth between 1.70 m to 10.49 m below the land survey datum.

Next, Landsat 8 data provided by the Malaysian Space Agency (MYSA). On 29th June 2017, the Landsat 8 data was acquired (extent: 56-row x 126 columns) at 03:21:23 (Greenwich Mean Time) and this data has been calibrated and orthorectified using Global Land Survey 2000 (GLS 2000) ground control points and Digital Elevation Model (DEM) [20]. In continuation, Landsat 8 has two push-broom instruments which are Operational Land Imager (OLI) and the Thermal Infrared Sensor (TIRS), total up eleven bands and each band serves a particular purpose. For the OLI sensor, the bands include eight multispectral bands with 30 m spatial resolution and one panchromatic band with 15 m spatial resolution. While the TIRS sensor, two thermal infrared spectral bands with 100 m spatial resolution.

Then, the Department of Survey and Mapping Malaysia (DSMM) provide tidal at Cendering, Terengganu, Malaysia with latitude: 05°15'50" N and longitude: 103°11'03" E. The data from the Cendering tidal station consisted of one-hour tidal interval readings with standard deviations of ± 26.7 mins (predicted time) and ± 14.1 cm (predicted height) [17].

Preparation of Newly Generated Calibration Data

SBES data consists of 18283 with a range of depth between 1.70 m to 10.49 m below the land survey datum, whereby 13.4% (6.66 km^2) of the extended area (49.69 km^2) has covered by SBES data. SBES points in the red region are divided into two sets of data: calibration data and evaluation data. Calibration data cover 60% of the evaluation area, and these data comprised 11191 SBES points used at the SDB computation process. While the evaluation data cover the whole SBES data, comprised 18283 SBES points, used in the bathymetry accuracy assessment.

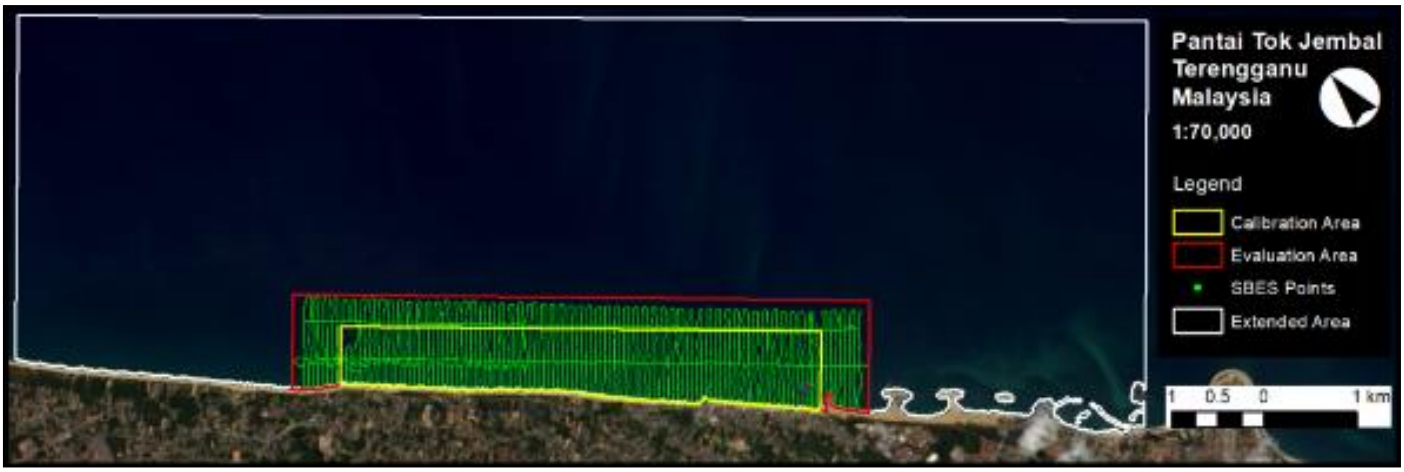

Figure 2. Showing the illustration of the Calibration data in the Calibration Area (yellow region) comprised 11191 SBES points, Evaluation data in the Evaluation Area (red region) comprised 18283 SBES points, and Extended Area (white region), the target size in generating SDB

The preparation of newly generated calibration data by first interpolating the calibration data using spatial predictors. Second, the raster output created from the interpolation process then converts into the point shapefile. Third, intersect function use to eliminate the point whereby not in the domain. Then, the newly generated calibration data ready to apply at the SDB computation process, generating SDB. When creating the output file in each step, there would be a shifting position of about 4 m. Hence, to avoid shifting, it is advising to set the environment setting as the original extent, thus, output with the same extent produces. Also, the gridding size must equivalent to Landsat images resolution, to ensures one data point fixated at the centre in each pixel.

1. Spatial Predictors

There are six spatial predictors use in interpolating the Calibration data, namely Inverse Distance Weightage (IDW), Universal Kriging (KRG), Thin-plate Spline (TPS), Spline with Tension (ST), Natural Neighbor (NN), and Topo to Raster (T2R). Furthermore, each spatial predictor works differently, depending on the sample of data, i.e., scattered or well distributed and mathematical approach including the parameter use.

1.1. Inverse Distance Weightage (IDW)

IDW is an exact approach that enforces the condition that defines the importance of a point more affected by known points nearby than points farther apart [4], [28]-[29], [40]. IDW calculates the predicted value by averaging all known quantities and adding more weight to closer points [28]. The Equation (1) generation for the IDW method is:

$$z_0 = \frac{\sum_{i=1}^{s} z_i \frac{1}{d_i^k}}{\sum_{i=1}^{s} \frac{1}{d_i^k}} \qquad (1)$$

Where z_0 is a value measured at points 0, z_i is the z value at a known point i, d_i the difference between points i and point 0, s the number of known points in the approximation used is, and k is the defined power that regulates the degree of local influence [4]. The quality of the IDW interpolation result depended on the good distribution of known points. When the known points are well-distributed, IDW provides good results [30]; when the distribution of sample data points is uneven, the result will be the opposite [4]. As in [28], one of the studies that use the IDW interpolation method. The study found that IDW is the most suitable and accurate method for the generation of river bathymetry. In another study conducted by [5], the generation of Digital Elevation Model (DEM) for the lower Athabasca River using two spatial interpolation techniques of IDW and Ordinary Kriging (OK), the result found that both produced similar results when compared.

1.2. Radial Basis Function (RBF): Thin-plate Spline (TPS) and Spline with Tension (ST)

RBF applies to a broad number of interpolation methods. The selection of the basis's function or equation determines how the surface fits between the control points. The RBF method has a parameter that controls the smoothness of the surface produced [4], [40]. A previous study by [40] has conducted a multiple spatial interpolation technique, including IDW, OK, RBF, and Local Polynomial Interpolation, and the study aimed to find the best spatial interpolation from cross-sectional sounding measurements for mapping river bathymetry. The findings showed that both RBF and Ordinary Kriging with Anisotropy (OKA) performed the best in bathymetry mapping.

Five RBF methods are available under the Geostatistical Analysis Toolbox. TPS and ST choose for this study. TPS for spatial interpolation is conceptually similar to splines for line smoothing, but TPS applies to surfaces rather than lines. This technique provides a surface that moves through the control points and at all points has the least possible change in slope. This approach, therefore, suits the control points with minimal surface curvature [4]. The TPS approximation Equation (2) is as follows:

$$Q(x,y) = \sum A_i d_i^2 log d_i + a + bx + cy \quad (2)$$

Where $x\ and\ y$ are the coordinates of the point to be interpolated, $d_i^2 = (x - x_i)^2 + (y - y_i)^2$, and $x_i$and y_i are the $x\ and\ y$ coordinates of control point i. TPS consists of two components, and the first $(a + bx + cy)$ represents the local trend function, which has the same form as a linear or first-order trend surface. Meanwhile, the second component, $d_i^2 log\ d_i$, represents a basis function, which is design to obtain minimum curvature surfaces. Furthermore, the coefficients $A_i, a, b, and\ c$ determines by a linear system of equations.

Unlike the IDW process, the TPS predicted values are not confined within the range of maximum and minimum values of the known points. The steep gradients in data-poor areas are a huge TPS concern and are often referred to as overshoots. TPS with tension enables the user to control the tension on the edges of the surface to pull [4]. Equation (3) for TPS with tension is:

a+ i=1nAiR(di) (3)

Where a represents the trend function, and the basis function $R(d)$ is as shown in Equation (4):

$$-\frac{1}{2\pi\varphi^2}[ln\left(\frac{\mathrm{d}\varphi}{2}\right) + \mathrm{c} + \mathrm{K}_0(\mathrm{a})] \quad (4)$$

Where φ is the weight to be used with the tension method, and if φ is set too close to zero, the approximation for ST is similar to the primary TPS method. A larger φ value reduces the plate's stiffness and, hence the range of the interpolated values, with the interpolated surface resembling the shape of a membrane passing through the control points. The effects of the TPS and ST interpolation affect the number of known points and the weight parameter. The greater the defined number of points, the greater the impact of distant points, and the smoother the interpolated surface [1].

1.3. Universal Kriging (KRG)

Kriging is a form of spatial interpolation for geostatistics. This method differs from other interpolation strategies, as Kriging can determine the accuracy of the prediction with estimated prediction errors. Universal Kriging assumes that the spatial variations in the z values have a drift or trend, apart from the spatial correlation between the sample point [4], [11], [40]. Besides, Universal Kriging typically incorporates a polynomial of the first order or the second order in the kriging process [4]. The Equation (5) of Universal Kriging linear-drift is:

$$M = b_1 x_i + b_2 y_i \quad (5)$$

Where $M$is the drift, x_i and y_i are the $x\ and\ y$ coordinates of sampled point i, and b_1 and b_2 are the drift coefficients. Higher-order polynomials do not recommend for two reasons, first, after the trend removal, Kriging is performed on the residual to assess the uncertainty; a higher-order polynomial will leave little variation in the residuals. Second, higher-order means a larger number of $b_i$coefficients to estimate along with the weights and a broader set of equations to be solved simultaneously [4].

Kriging assumes that the space studies are stationary; that is, the joint probability distribution does not change throughout the study space. It also assumes a property called isotropy; that there is uniformity in every direction. If these conditions are challenging to fulfil, the method becomes problematic. However, in Universal Kriging, the stationary requirement is relaxed. The model's accuracy will be limited if the data are not spatially correlated, if limited in the spread, or if the number of data points is small [14].

Universal Kriging is the interpolator with the anisotropic condition, which is highly suggested based on the previous studies. As stressed by [6] and [40], the methods that account for the anisotropic nature of the riverbed and submerged relief, i.e. the preferential direction of the variability of bathymetric performance, should be compared, with greater weight given to the direction with the significant influence. In [40] study proved that when compared Elliptical Inverse Distance Weightage, Universal Kriging, and Ordinary Kriging with Anisotropy (the interpolators with the anisotropic condition) to IDW or Ordinary Kriging (isotropic interpolators), the interpolators with anisotropic condition gives a slightly better result, which is >5% to 20% reduction in root mean square error (RMSE) values.

1.4. Natural Neighbour (NN)

The NN interpolation tool calculates the nearest sub-set of samples to a question point and uses weights to points based on the proportionate regions interpolating value. The technique is known as Sibson interpolation or 'area stealing' is local and uses only a subset of samples around the point of the question. This means that the interpolated heights are within the range of the used samples. NN does not deduce trends and does not establish hills, troughs, ridges or valleys not represented already by input samples. The surface passes through the input samples and is smooth in every position, except where the input samples are located. When compare distance-based interpolator tools such as IDW apply the same weights to the most northern and northeast points based on their identical distance from the point of interpolation. Nevertheless, NN interpolation assigns weights of 19.12% and 0.38% to the northernmost point and the north-eastern point, respectively, based on the overlap percentage [9]. NN is a different method in which it does not extrapolate values, resolving the interpolation only inwards data domain [29]. As [29] has been explained in detail this method.

1.5. Topo To Raster (T2R)

The T2R is an interpolation method designed specifically to create hydrologically accurate digital elevation models (DEMs). It is based on Michael Hutchinson's Australian National Digital Elevation Model (ANUDEM) program (1988, 1989, 1996, 2000, 2011). The T2R interpolation method is designed to take advantage of the common input data types and the known characteristics of the elevation surfaces. This approach uses a technique to interpolate finite differences iteratively. Without sacrificing the superficial consistency in global interpolation methods such as Kriging and Spline, the

computational efficiencies of local interpolation methods such as IDW interpolation are optimized. T2R is a discerning TPS technique for which the roughness penalty is amended, allowing the fitted DEM to track sudden changes in terrain such as streams, ridges and cliffs [10]. The difference defines as the first and second degree of partial derivation f of the interpolation method described by the following Equations (6), (7), and (8):

$$J_1(f) = \int (f_x^2 + f_y^2) dxdy \qquad (6)$$

$$J_1(f) = \int (f_{xx}^2 + f_{xy}^2 + f_{yy}^2) dxdy \quad (7)$$

To remove the maximum and minimum peak effect (excessively smooth or peaked soil) and to achieve a practical surface terrain J_1 and J_2 must be minimized. A very smooth surface is obtained if only J_2 is minimized, and vice versa, if only,J_1 is minimized, maximum and minimal peaks occur [2], [10]. [35] propose that a roughness penalty is imposed when taking the cell resolution into account.

$$J(f) = 0.5h^{-2} J_1(f) + J_2(f) \quad (8)$$

Essentially, T2R is a combined form of interpolation that uses a discrete technique based on degree m and k smoothness spline polynomial functions, where the roughness can be changed to allow DEM to be produced with sudden changes in the ground, such as areas affected by tides, ridges or cliff depths. Area maximums or local minimums are sometimes considered these landforms. Of the present tense, point elevation features are used.

Furthermore, [2] one of the studies that use the T2R interpolation method. The study aimed to test four interpolation methods to identify the most appropriate method, which would give an accurate description of the riverbed, based on single-beam bathymetric measurements. The four interpolation techniques selected were IDW, RBF, KRG, and T2R. The findings showed that T2R has the best performance and the most accurate interpolation method to be used when creating a DEM for a given number of points and grid, the result closely followed by the KRG, RBF, and IDW.

Pre-processing Stage

The bathymetry derivation process initially begins with pre-processing stage and three-step involves includes pan-sharpening, subsetting and atmospheric correction.

First, the pan-sharpen process of Landsat images conducted by merging 15 m resolution panchromatic data with 30 m resolution multispectral data. The low spatial resolution spectral band must fall within the panchromatic band. Otherwise, the images will not be included in the resampling process. Other than that, both multispectral and panchromatic data must be in the same projection to ensure both images are aligned in the same position. The pan-sharpening processing undertaken to improve the information extraction [27]. Besides, the effect of pan-sharpening is best on images with homogenous surface features such as a flat desert or water surface, an advantage in this research since it focuses on the water surfaces [15].

Next, subset the image according to the area and position of the created region of interest (ROI). This strategy to focuses on the area of research, reduces the workload of an entire image [23], reducing time and enhancing productivity.

Then, the atmospheric correction was conducted to improve the depth model's performance and minimize the atmospheric effects that alter the actual radiance data, whereby the satellite sensor's actual representation [3]. Dark Object Subtraction (DOS) assumes that dark objects reflect no light and that any values greater than zero must be due to atmospheric scattering. By subtracting these values from each pixel in the band, the scattering is eliminated. On the Landsat image, a dark subtraction was performed on an area of deep oceanic pixels [16]. The limitation of this step due to the presence of a cloud covers the information underneath and creates a shadow pixel. The shadow pixel appears dark colour pixel, which can mistake as an oceanic pixel. DOS atmospheric correction only removes the scattering and brightening the images. This method is ineffective in removing cloud, cloud shadow, and haze. However, since the cloud and haze are less present in the Landsat images, thus, less effect on the bathymetry performances.

SDB Computation

The newly generated calibration data are applied under this stage. The depth retrieval using Log-ratio Transform method, by first, rationing natural logarithm $(\ln)$ blue against$\ln$ green band. Second, linear regression performed between the depth of newly generated calibration data and the $\ln$ blue-green ratio value. Third, the equation of Z structured from the regression line and m_0 and m_1 values obtained. Forth, SDB computes using the complete structure of the Z equation. The depth estimation Equation (9) is as follows:

$$Z = m_1 * \frac{ln\,(nL(\lambda_2))}{ln\,(nL(\lambda_1))} - m_0 \qquad (9)$$

Where:

Z = depth estimation,

n, m_1 and m_0 = the constant-coefficient for the model, and

$L(\lambda_1)$ and $L(\lambda_2)$ = reflectance for spectral λ_1 and λ_2.

Log-ratio Transform method limited success in high variable bottom type [12], which not in the case of Pantai Tok Jembal, since this study area is a sandy bottom type. Besides, although this area prone to erosion, luckily, the water condition at this area still in good condition. This is because, during the satellite images capture on 29th June 2017, during the southwest monsoon, which is the dynamic ocean not strong as during northwest monsoon. Thus, the disturbances from substances suchlike sediment in blue-green-ratio not significantly high and the Log-ratio Transform method still reliable to use in this type of water condition.

In continuation, tidal data used under this section to bridge the time gap and vertical datum. Tidal correction conduct before and after SDB obtain and it is because SBES data originally from Mean Sea Level (MSL) and the Landsat

image capture during the tide presence. Initially add tide value to the newly generated calibration data, before applying this data at the SDB computation process. After the SDB computation process performs and the SDB produced, SDB needs to subtract with tide values to reduce the depth of SDB back in MSL. Finally, the final step is masking. The masking function separates the water pixel from the land pixel since the SDB focuses on the water area.

Data Analysis

Under this section, evaluation data comprised 18283 SBES points used to validate the SDB generated from Landsat 8 images using the Log-ratio Transform method. The statistical analysis conducted is Root Mean Square Error (RMSE) and coefficient determination (R^2) between SDB and evaluation data, along with maximum depth, minimum of depth, an average of depth, and standard deviation. Besides, there are three stages of analysis conducted connecting the objective in this research: firstly, evaluate the pattern error of spatial prediction in the production of newly generated calibration data. Secondly, the evaluation of SDB generated using newly generated calibration data. Thirdly, evaluate the result of accuracy assessment of SDB at the extended area.

Result & Discussion

Preparing the Newly Generated Calibration Data

Figure 3 below shows the irregular space of calibration data in the calibration area (yellow region), with a void area before the interpolation process conducted. Six spatial predictors, namely, Inverse Distance Weightage, Universal Kriging, Thin-plate Spline, Spline with Tension, Natural Neighbour, and Topo to Raster, were used to interpolate the calibration data.

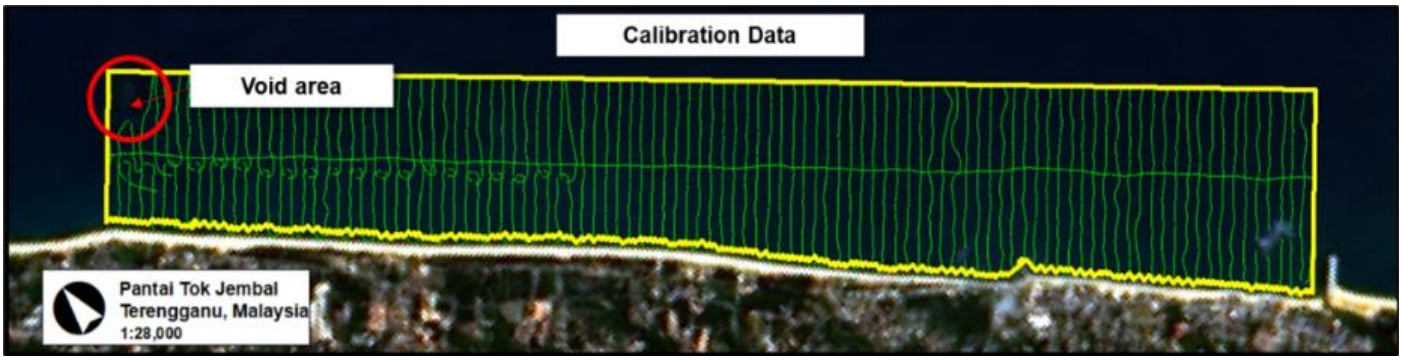

Figure 3. showing the Calibration data before interpolation carry out

Table 1. Summary of parameters used in the spatial interpolation method used to interpolate calibration data

Parameterization	Method
Output cell size: 15 m, Power: 2, Search radius (optional): variable, Number of points: 12	IDW
Output cell size: 15 m, Universal Kriging method: universal, Semi-variogram model: linear with linear drift, Search radius (optional): variable, Number of points: 12	KRG
Output cell size: 15 m, Search Neighbourhood (optional): standard, major semiaxis, and minor semiaxis is automatic, Angle: 0, RBF: Thin-plate Spline	TPS
Output cell size: 15 m, Spline type: tension, Weight: 0.1, Number of points: 12	ST
Output cell size: 15 m	NN
Output cell size: 15 m	T2R

Interpretation of Table-1

The raster output produces under the interpolation process based on the stated parameter and the different number of parameter use depending on the spatial interpolation method. Also, these parameters determine the raster outcomes.

After the six interpolation methods were successfully carried out, the results were six raster output with a different interpolation pattern, as illustrated in Figure 4. Next, the evaluation process was conducted on the six raster output using the evaluation data and the validation results, which also can be found in Figures 4 and 5.

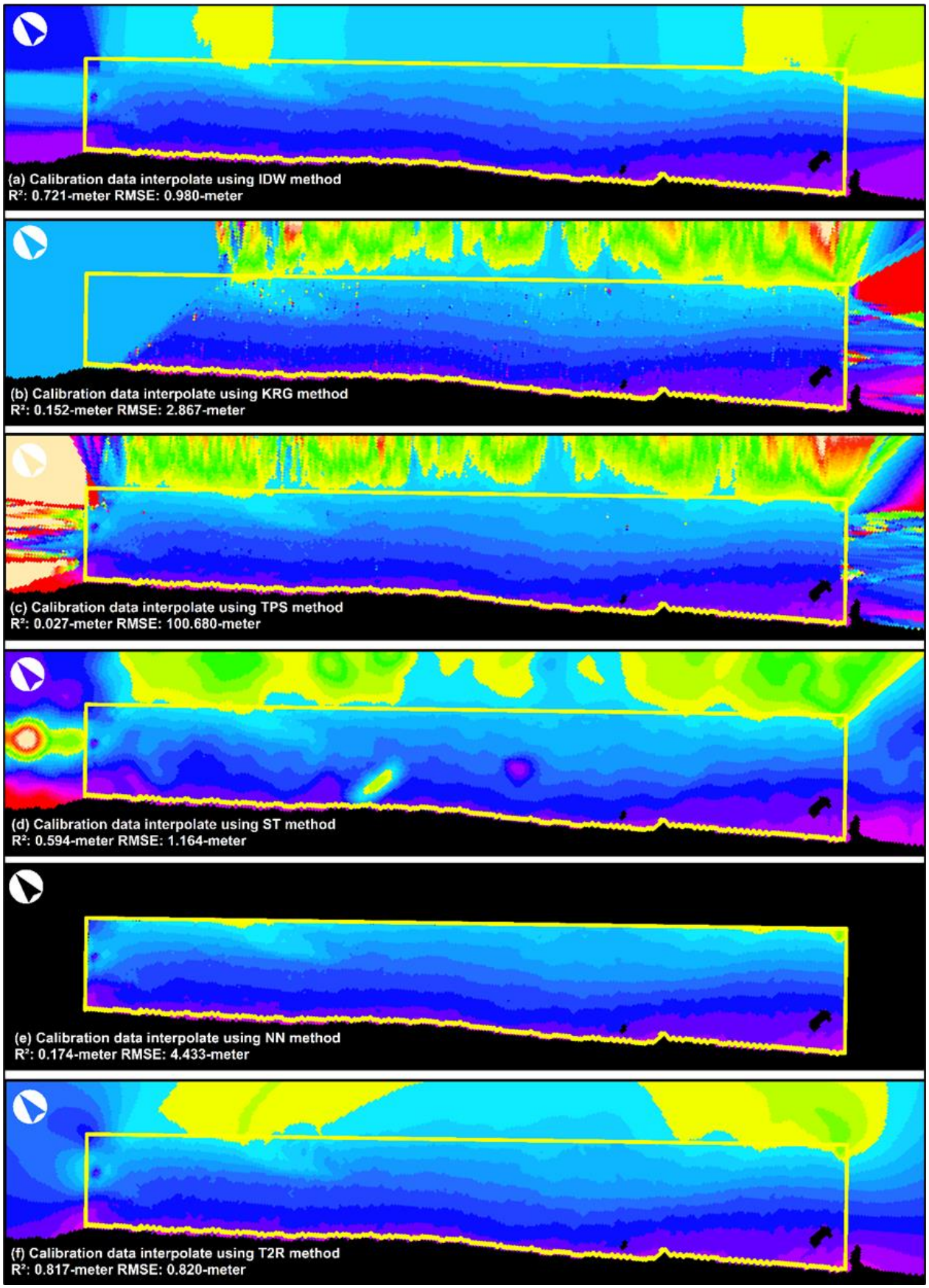

Figure 4. Showing the raster output produced after applying six spatial predictors on the calibration data: (a) SBES Interpolated – Inverse Distance Weightage (b) SBES Interpolated – Universal Kriging (c) SBES Interpolated – Thin-plate Spline (d) SBES Interpolated – Spline with Tension (e) SBES Interpolated – Natural Neighbor and (f) SBES Interpolated – Topo to Raster

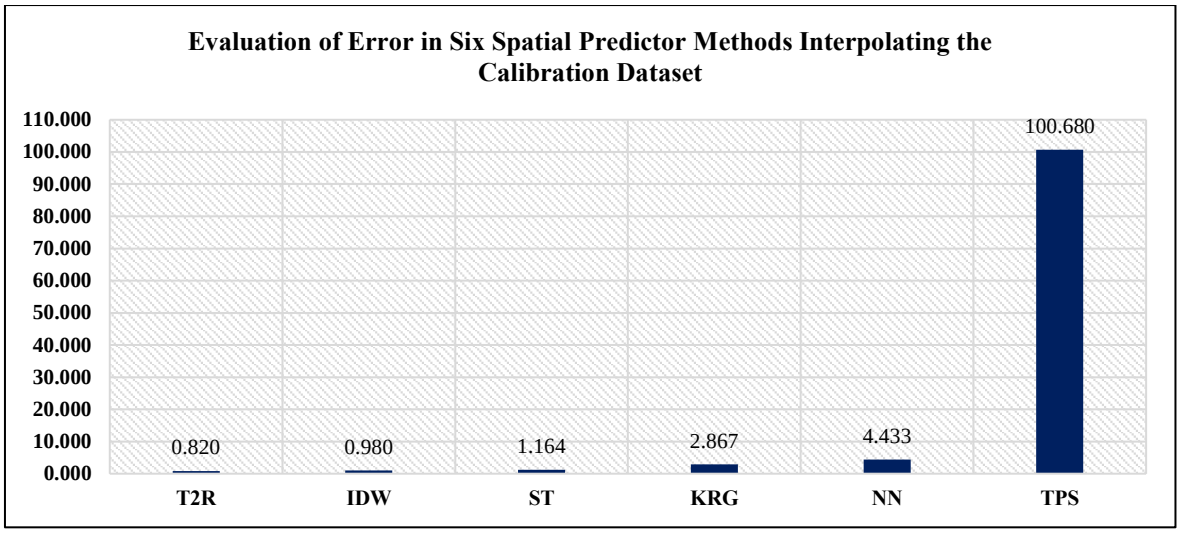

Figure 5. Showing the evaluation of error graph for six spatial predictor methods interpolating the calibration data: Topo to Raster (T2R), Inverse Distance Weightage (IDW), Spline with Tension (ST), Universal Kriging (KRG), Natural Neighbor (NN), and Thin-plate Spline (TPS)

Based on Figures 4 and 5, evaluation of error in six raster output produced after applying six spatial predictors on the calibration data. The results showed that the Topo to Raster interpolation technique gave a satisfactory result with the lowest RMSE value (0.820 m). This finding is similar to those in earlier studies [2] in which the Topo to Raster method has consistently given satisfactory results in the interpolation process.

The Inverse Distance Weightage method has a limitation in the range of maximum and minimum values of the known points, while Thin-plate Spline and Spline with Tension under the RBF do not, for the surface smoothing concept. When Inverse Distance Weightage compares with the RBF method, the results indicated that Inverse Distance Weightage (RMSE: 0.980 m) performed significantly better than Thin-plate Spline (RMSE: 100.680 m) and better than Spline with Tension (RMSE: 1.164 m).

The major problem in Thin-plate Spline is that it tends to overshoot, especially in low data areas. To overcome this problem, the Spline with Tension method use to correct the overshoots that occur. This method allows the user to control the tension to pull on the edge of the surface. As presented in Figure 5, the Thin-plate Spline without the tension produced an RMSE of 100.680 m, but when tension was applied, the RMSE value lowered to 1.164 m (Spline with Tension).

Next, the Universal Kriging method produced a significantly better result than Natural Neighbour and Thin-plate Spline with an RMSE of 2.867 m. This method is recommended [6] and [40]because it considers the anisotropic nature in the bathymetric data during interpolation, which is essential. At the same time, the Natural Neighbour interpolation method (RMSE = 4.433 m) produced a significantly better result than the Thin-plate Spline. Even though this method is useful in local interpolation, it is not practical for extrapolating, because this method does not extrapolate values and only interpolates the data domain inwards [39].

In continuation, after interpolating the SBES point in the calibration data, the raster output produces from the interpolation process, i.e., IDW, TPS, ST, KRG, NN, and T2R, then convert into the point shapefile. Then, intersect function use to eliminate the point whereby not in the domain. Finally, the newly generate calibration data ready to apply at the SDB computation process, generating SDB. Based on Figure 6 shown the newly generated calibration data. The difference between the new calibration data and the older calibration data (Figure 3) was the SBES points arrangement. In the newly generated calibration data, the SBES points systematically arranged. Thus, this will facilitate pixel-to-point extraction value, whereby one pixel represented one point, hence, there will be no pixel left out during the extraction process.

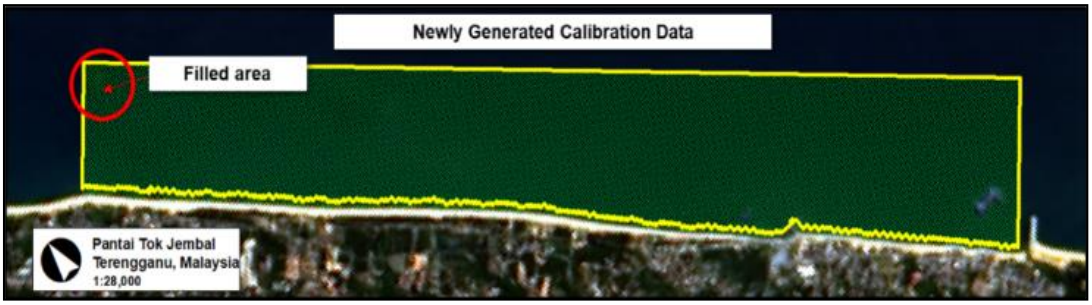

Figure 6. Showing the Calibration data after interpolation carry out

SDB Computation

For computing the SDB, the regression process conducted between depth of newly generated calibration data and the ratio of ln Blue to ln Green to obtain the m_0, m_1. Then, after all the values obtained and the Z equation complete structured, Z can be computed.

Table 2. Summarize the m_0 and m_1 value and the complete structure of the equation to compute Z by each method

Newly generated calibration data	m_0	m_1	Equations to compute Z resulting from regression line between depth of newly generated calibration data and the ratio of Ln Blue to Ln Green.
IDW	-1.01	5.41	$Z = -1.01 * ((x - 0.51) / 0.0604) - 5.41$
KRG	-1	5.4	$Z = -1 * ((x - 0.51) / 0.06) - 5.4$
TPS	-0.986	5.29	$Z = -0.986 * ((x - 0.51)/0.0604) - 5.29$
ST	-0.99	5.5	$Z = -0.99 * ((x - 0.51)/0.06) - 5.5$
NN	-17.092	3.3119	$Z = -17.092 * (x) + 3.3119$
T2R	-1	5.4	$Z = -1 * ((x - 0.51) / 0.06) - 5.4$

[a]x = the reflectance value from rationing ln Blue and ln Green

[b]Z = SDB

Interpretation of Table-2

The obtaining valuem_0 and m_1 value complete the Z equation and the Z equation differ in each set of newly generated calibration data, thus, there will be distinct in SDB result.

By using the equation as presented in Table 2, SDB generated in an extended area of 49.69 km². The result of SDB using the newly generated calibration data shown in Figure 7.

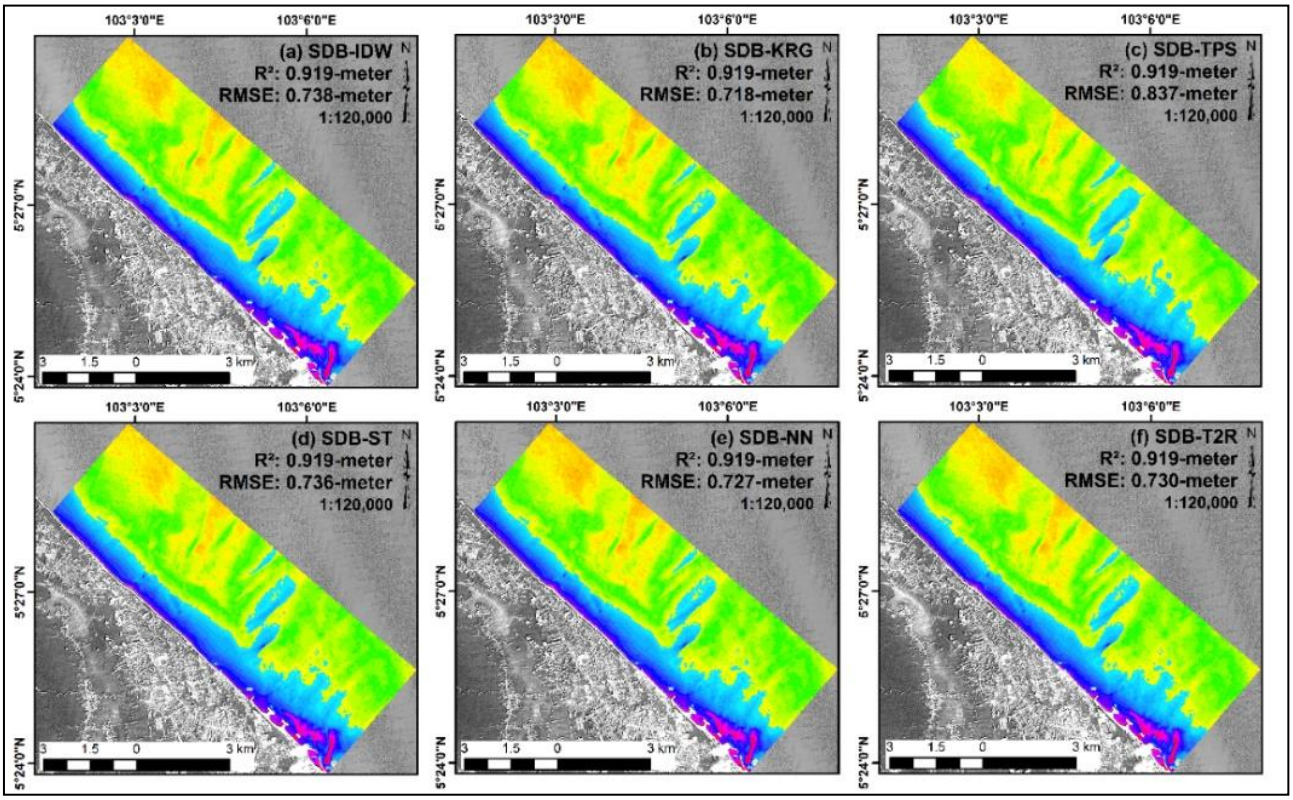

Figure 7. Illustrates the six SDB results generated from Landsat 8 using the log-ratio transform method and calibrated using each different newly generated calibration data. The colours depicted on the bathymetric mapping indicates the depth contour, and all the SDB results showed a slightly similar depth contour pattern.

Bathymetry Accuracy Assessment

Comparative analysis conduct between the six SDB results generated each different newly generated calibration data. The accuracy of SDB then assesses using two statistical indices, i.e., R^2 and RMSE. The summarise results in Table 3.

The R^2 for the regression model of log-ratio transform calibrate with six newly generated calibration data and all the SDB results gave a similar value of 0.919 m, which is high. The obtain high value of R^2 is because the regression model accounts for more of the variance, in which the data points are closer to the regression line. As presented in Figure 8,

shows the scatter plots between bathymetry from SDB and bathymetry from evaluation data.

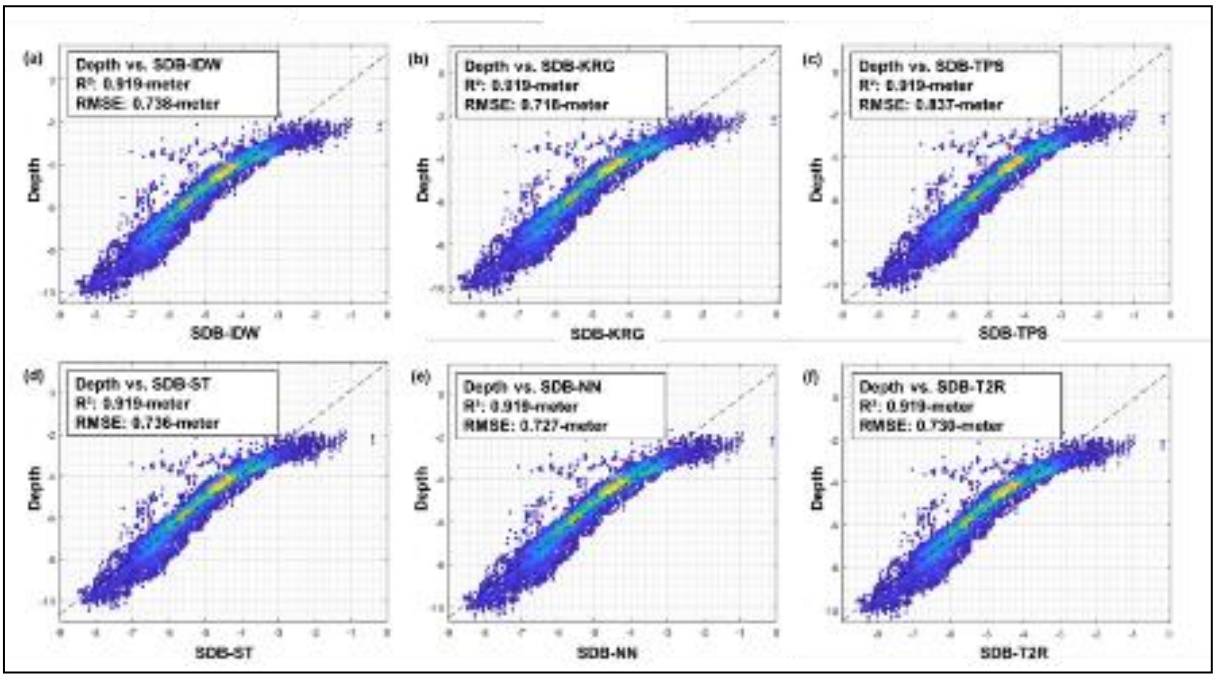

Figure 8. Showing the two-dimensional scatter plots between bathymetry from evaluation data and bathymetry from SDB calibrate using six newly generated calibration data: (a) Inverse Distance Weightage, (b) Universal Kriging, (c) Thin-plate Spline, (d) Spline with Tension, (e) Natural Neighbour and (f) Topo to Raster.

Table 3. Statistical results of SDB generated using the six Newly Generated Calibration Data

	SDB-IDW	SDB-KRG	SDB-TPS	SDB-ST	SDB-NN	SDB-T2R	SBES
RMSE	0.738	0.718	0.837	0.736	0.727	0.730	
R^2	0.919	0.919	0.919	0.919	0.919	0.919	
Min	-8.516	-8.616	-8.281	-8.465	-8.575	-8.546	
Max	-0.218	-0.079	-0.218	-0.403	-0.133	-0.187	-1.70
Mean	-5.133	-5.135	-4.994	-5.178	-5.133	-5.138	-10.49
Median	-5.134	-5.136	-4.995	-5.179	-5.134	-5.139	-5.52
SD	1.269	1.306	1.233	1.233	1.291	1.279	
Cal. Pts	17061						
Eva. Pts	18283						

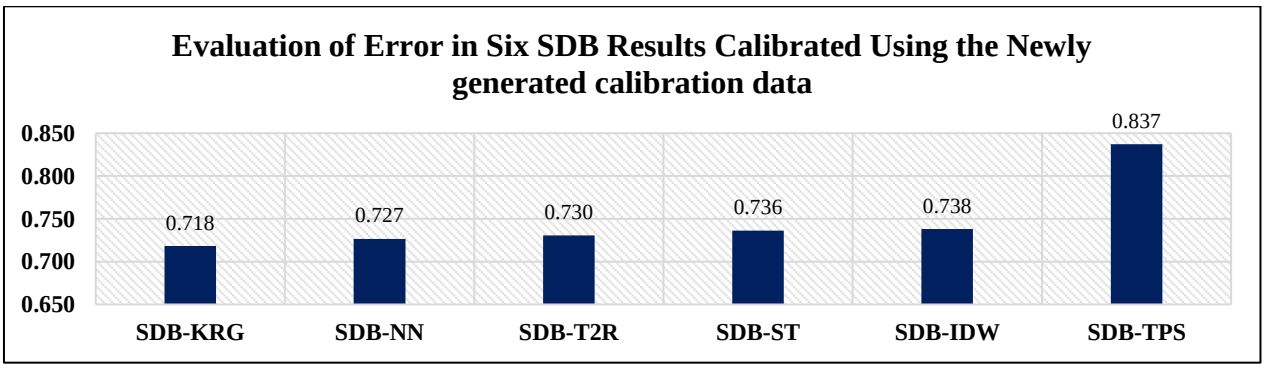

Figure 10. Showing the evaluation of error graph for six SDB results calibrated using the newly generated calibration data: Universal Kriging (SDB-KRG), Natural Neighbor (SDB-NN), Topo to Raster (SDB-T2R), Spline with Tension (SDB-ST), Inverse Distance Weightage (SDB-IDW), and Thin-plate Spline (SDB-TPS).

Interpretation of Table-3

The results showed an increase in the RMSE value from SDB-KRG (0.718 m), SDB-NN (0.727 m), SDB-T2R (0.730 m), SDB-ST (0.736 m), SDB-IDW (0.738 m) to SDB-TPS (0.837 m). Nevertheless, the results showed a significantly small difference except for SDB-TPS. The SDB-KRG method gave the lowest RMSE value of 0.718 m; therefore, SBD-KRG produced the best result. Furthermore, each method shows

improvement from bathymetry that depends only interpolation process to the bathymetry from SDB that calibrates using new calibration data. The improvement can be seen first, from SDB-KRG improves 76.7%, second, SDB-NN improves 74.5%, third, SDB-T2R improves 10.2%, fourth, SDB-ST improves 32.5%, and fifth, SDB-IDW improves 19.8% and sixth, SDB-TPS improves 89.2%.

Conclusion

This paper present coastal depth extraction from satellite images. The problem faces when the irregular space of SBES data and the 15 m resolution of Landsat imager after pan-sharpening causes more than one SBES point with different depth value to fit into one Landsat pixel, and because of this problem, create uncertainty. Besides, the unintended 'holes' within the SBES data, reducing quite an amount of data, which is essentially needed, since SBES data use as ground truth data. Therefore, the solution is by using the spatial interpolation method to recreate the SBES points into uniformly spaces, long and dense data, then applied at SDB computation process.

As expected, each spatial predictor works differently when compared to many related studies. The interpolation depended on the focus area, type of sample use, sample size and forth. Besides that, the interpolation process also concerning the parameterization setting. When undergoing the interpolation process, the suitable option must be identified carefully because the outcomes are produced depending on the parameterization setting, which not in the case of this study, since the parameterization choose by default. Moreover, the effectiveness of spatial predictors depends on how well the known points distribution, the amount and also the quality of the data used. In the case of data distribution, where the known data are farther away than the predicted data, will be less influence, and the error will increase.

Next, the task of spatial predictors is very helpful in solving the problem related to space, distribution and quantity of the SBES data. The recreation uniform spaces of SBES data in ensuring that each Landsat pixel represents one correct value of SBES point and the value generated using the mathematical algorithm of the spatial predictors. For example, given the scenario where five SBES points are close together located in a one-pixel box, a mathematical formula from spatial predictor calculates and determines one value representing the pixel. Also, since each pixel represented with one SBES point, thus, no pixel was left out during the pixel to point extraction. Other than that, the interpolation process increase the number of bathymetry points and the addition of data especially at the area where the 'holes' located, thus, the uniform space and long data help refine the bathymetry derivation process.

Comparative analysis shows the result of SDB when using a different set of newly generated calibration data, and based on the result indicates that the method gives a significantly small difference between the adjacent method, except for the SDB-TPS. Therefore, any method that can be used, except for Natural Neighbor, need to be aware of the limitation which is this method cannot extrapolate outside the calibration area. Furthermore, there is an improvement in bathymetry from SDB that calibrates using new calibration data when compared with a bathymetry that depends only interpolation process.

To summarise, this study has successfully attained the research objectives by utilizing the newly generated calibration data in generating SDB of the extended area. The task of spatial interpolation recreates the SBES data from irregular space and short data to uniform space and long data, which facilitate in pixel to point value extraction and help refine the bathymetry derivation process. Furthermore, the proposed method suitable to be used when the data are not applicable or limited.

References

Amante, C.J., & Eakins, B.W. (2016). Accuracy of Interpolated Bathymetry in Digital Elevation Models. *Journal of Coastal Research,* 76, 123–133. https://doi.org/10.2112/si76-011

Arseni, Voiculescu, Georgescu, Iticescu, & Rosu. (2019). Testing Different Interpolation Methods Based on Single Beam Echosounder River Surveying. Case Study: Siret River. *ISPRS International Journal of Geo-Information,* 8(11), 507. https://doi.org/10.3390/ijgi8110507

Chakravortty, S., & Chakrabarti, S. (2011). Preprocessing of Hyperspectral Data: A case study of Henry and Lothian Islands in Sunderban Region, West Bengal. *India. Int. Journ. Geom. Geosc,* 2, 490–501.

Chang, K.T. (2008). *Introduction to Geographic Information System Fourth Edition.* McGraw-Hill.

Chowdhury, E.H., Hassan, Q.K., Achari, G., & Gupta, A. (2017). Use of bathymetric and LiDAR data in generating digital elevation model over the Lower Athabasca River Watershed in Alberta, Canada. *Water (Switzerland),* 9(1). https://doi.org/10.3390/w9010019

Curtarelli, M., Leão, J., Ogashawara, I., Lorenzzetti, J., & Stech, J. (2015). Assessment of spatial interpolation methods to map the bathymetry of an Amazonian hydroelectric reservoir to aid in decision making for water management. *ISPRS International Journal of Geo-Information,* 4(1), 220–235. https://doi.org/10.3390/ijgi4010220

El-Hattab, A.I. (2014). Single beam bathymetric data modelling techniques for accurate maintenance dredging. *Egyptian Journal of Remote Sensing and Space Science,* 17(2), 189–195. https://doi.org/10.1016/j.ejrs.2014.05.003

Emery, W.J., & Thomson, R.E. (2001). Chapter 3 - Statistical Methods and Error Handling. In W.J. Emery & R.E. Thomson (Eds.). *Data Analysis Methods in Physical Oceanography,* 193–304. https://doi.org/https://doi.org/10.1016/B978-044450756-3/50004-6

ESRI. (2012). *How Natural Neighbor works.* 11–12.

ESRI. (2013). *Topo to Raster (Spatial Analyst).* 2013 (6/20/2013), 6–11.

Firdaus, N., and Talib, S.A. (2014). *Spatial Interpolation of Monthly Precipitation in Selangor,* Malaysia - Comparison and Evaluation of Methods.

Geyman, E., and Maloof, A. (2019). A Simple Method for Extracting Water Depth from Multispectral Satellite Imagery in Regions of Variable Bottom Type. *Earth and Space Science,* 6. https://doi.org/10.1029/2018EA000539

Gholamalifard, M., Sari, A.E., Abkar, A., and Naimi, B. (2013). and Principal Components Analysis (PCA) in Southern Caspian Sea. *International Journal of Environmental,* 7(4), 877–886.

Glen, S. (2018). Kriging: Definition, Limitations.

Harris Geospatial Solutions. (2020). *Gram-Schmidt Pan Sharpening.*

Hernandez, W., and Armstrong, R. (2016). Deriving Bathymetry from Multispectral Remote Sensing Data. *Journal of Marine Science and Engineering,* 4(1), 8. https://doi.org/10.3390/jmse4010008

Jadual Ramalan Air Pasang Surut (Tide Prediction Tables) Malaysia 2017. (2017). Kuala Lumpur: Department of Survey and Mapping Malaysia.

Jaharudin, P., Kamarul, M.D., Abu, T.J., Haslina, M., and Pravinassh, R. (2019). Impact of coastal erosion on local community: Lifestyle and identity. *Disaster Advances,* 12(2), 19–27.

Kanno, A., Koibuchi, Y., and Isobe, M. (2011). Shallow Water Bathymetry from Multispectral Satellite Images: Extensions of Lyzenga'S Method for Improving Accuracy. *Coastal Engineering Journal,* 53(04), 431–450. https://doi.org/10.1142/S0578563411002410

Landsat Level-1 Processing Details. (n.d.). June 5, 2020, https://www.usgs.gov/land-resources/nli/landsat/landsat-level-1-processing-details

Manessa, M.D.M., Haidar, M., Hartuti, M., and Kresnawati, D.K. (2018). Determination of the Best Methodology for Bathymetry Mapping Using Spot 6 Imagery: a Study of 12 Empirical Algorithms. *International Journal of Remote Sensing and Earth Sciences (IJReSES),* 14(2), 127. https://doi.org/10.30536/j.ijreses.2017.v14.a2827

Mohamed, H., and Nadaoka, K. (2017). Assessment of machine learning approaches for bathymetry mapping in shallow water environments using multispectral satellite images. *International Journal of Geoinformatics,* 13(2), 1–15.

Najhan Md Said, Mohd Razali Mahmud, and Rozaimi Che Hasan. (2017). Satellite-derived Bathymetry: Accuracy Assessment on Depths Derivation Algorithm for Shallow Water Area. *ISPRS - International Archives of the Photogrammetry, Remote Sensing and Spatial Information Sciences, XLII-4/W5,* 159–164. https://doi.org/10.5194/isprs-archives-XLII-4-W5-159-2017

Najhan Md Said, Mohd Razali Mahmud, and Rozaimi Che Hasan. (2018). Evaluating satellite-derived bathymetry accuracy from Sentinel-2A high-resolution multispectral imageries for shallow water hydrographic mapping. *IOP Conference Series: Earth and Environmental Science,* 169(1). https://doi.org/10.1088/1755-1315/169/1/012069

Nur Syahirah Hashim, Othman Mohd Yusof, Windupranata, W., and Saiful Aman Sulaiman. (2020). Integration of Satellite-Derived Bathymetry and Sounding Data in Providing Continuous and Detailed Bathymetric Information. *{IOP} Conference Series: Earth and Environmental Science,* 618, 12018. https://doi.org/10.1088/1755-1315/618/1/012018

Nur Syahirah Hashim, Windupranata, W., and Saiful Aman Sulaiman. (2020). Shallow-Water Bathymetry Estimation Using Single Band Algorithm and Green Band Algorithm. *2020 11th IEEE Control and System Graduate Research Colloquium (ICSGRC),* 214–219. https://doi.org/10.1109/ICSGRC49013.2020.9232639

Pan-sharpening for improved information extraction. (n.d.). June 5, 2020. https://www.researchgate.net/publication/279611673_Pan-sharpening_for_improved_information_extraction

Pankalakr, S.S., and Jarag, A.P. (2016). Assessment of spatial interpolation techniques for river bathymetry generation of Panchganga River basin using geoinformatic techniques. *Asian Journal of Geoinformatics,* 15(3), 9–15.

Pavão, C.G., França, G.S., Marotta, G.S., Menezes, P.H.B.J., Neto, G.B.S., and Roig, H.L. (2012). Spatial Interpolation Applied a Crustal Thickness in Brazil. *Journal of Geographic Information System,* 04(02), 142–152. https://doi.org/10.4236/jgis.2012.42019

Salhi, A. (2018). *When can I use Kriging or IDW?*

Sarfin, R.L. (2020). *5 Characteristics of Data Quality.*

Smith, J.R., Kinsman, N.E.M., and Misra, D. (2012). *Using WorldView-2 Multispectral Bands for Shallow Water Bathymetric Survey near Wales,* Alaska Figure 1—Location of Wales in the state of Alaska. 254.

SONARLITE Portable Echo Sounder System (p. 2). (n.d.). Nautikaris.

Spectra Precision SP80 GNSS Receiver (p. 4). (n.d.). Spectra Precision.

Stein, J., Hutchinson, M.F., Xu, T., and Stein, J.A. (2011). Recent Progress in the ANUDEM Elevation Gridding Procedure Recent Progress in the ANUDEM Elevation Gridding Procedure. (JANUARY).

Teodoro, A.C., Almeida, R., and Gonçalves, M. (2014). Independent Component Analysis (ICA) performance to bathymetric estimation using high resolution satellite data in an estuarine environment. *Remote Sensing for Agriculture, Ecosystems, and Hydrology XVI,* 9239, 923915. https://doi.org/10.1117/12.2067196

Teodoro, A., and Pais-barbosa, J. (2010). *Bathymetric estimation through principal components analysis using IKONOS-2 data.* 7824, 1–9. https://doi.org/10.1117/12.864565

Tran, T.D., and Ho, T.H.M. (2016). Contribution of Satellite Altimetry Data in Geological Structure Research in the South China Sea. *ISPRS - International Archives of the Photogrammetry, Remote Sensing and Spatial Information Sciences,* XLI-B8(July), 1187–1190.

https://doi.org/10.5194/isprsarchives-XLI-B8-1187-2016

Wölfl, A.C., Snaith, H., Amirebrahimi, S., Devey, C.W., Dorschel, B., Ferrini, V., Wigley, R. (2019). Seafloor Mapping – The Challenge of a Truly Global Ocean Bathymetry. *Frontiers in Marine Science*, 6, 283.

https://doi.org/10.3389/fmars.2019.00283

Wu, C.Y., Mossa, J., Mao, L., and Almulla, M. (2019). Comparison of different spatial interpolation methods for historical hydrographic data of the lowermost Mississippi River. *Annals of GIS*, 25(2), 133–151. https://doi.org/10.1080/19475683.2019.1588781